Tellus SERIES A DYNAMIC METEOROLOGY AND OCEANOGRAPHY
PUBLISHED BY THE INTERNATIONAL METEOROLOGICAL INSTITUTE IN STOCKHOLM

Drivers of North Atlantic Oscillation Events

By IRIS MANOLA*, REINDERT J. HAARSMA and WILCO HAZELEGER,
Royal Netherlands Meteorological Institute, Wilhelminalaan 10, 3732 GK De Bilt, The Netherlands

(Manuscript received 20 September 2012; in final form 3 April 2013)

ABSTRACT

This work is set out to quantify the contribution of tropical and extratropical atmospheric forcing mechanisms to the formation of the North Atlantic Oscillation (NAO) pattern. Although the NAO varies on a wide range of time scales, we focus on 10–60 d. At these time scales, mechanisms are at play in the atmosphere that can generate the characteristic dipole pattern. We focus on the tropical Rossby Wave Source (RWS) and extratropical eddy activity. Anomalous tropical and extratropical vorticity forcing associated with the NAO is derived from atmospheric reanalysis data and applied in an idealised barotropic model. Also, using winds from composites of the NAO, the vorticity forcing is derived inversely from the barotropic vorticity equation. Both types of forcing are imposed in the barotropic model in the tropics and extratropics, respectively. An important result is that the tropics dampen the NAO as a result of a negative feedback generated in the extratropics. The damping is strongest, about 30%, for the negative phase of the NAO. For the positive phase, the damping is about 50% smaller. The results show that the barotropic vorticity equation can represent the dynamics of both tropical and extratropical forcing related to the formation of the NAO patterns.

Keywords: North Atlantic Oscillation, Rossby wave source, eddy activity, tropical forcing

1. Introduction

The North Atlantic Oscillation (NAO) is the major source of atmospheric variability over the Northeast Atlantic, Europe and North America (Branstator 2002). NAO plays an important role in the formation of the prevailing weather patterns and their day-to-day variations (Platzman, 1968). The NAO is predominantly generated by extratropical dynamics, which involves extratropical eddy fluxes, wave breaking activity and shifts in the storm tracks. In addition to that, the NAO is affected by tropical deep convection associated with sea surface temperature (SST) anomalies. However, the role of the tropical forcing in the development of the NAO pattern is yet to be fully clarified.

It is widely investigated and accepted that the NAO is primarily forced by extratropical atmospheric variability, such as the eddy activity and wave breaking (for instance, Feldstein, 2003; Thompson et al., 2003; Vallis et al., 2004). Results from model and observational studies by Franzke et al. (2003), Benedict et al. (2004), and Riviere and Orlanski (2007) indicate that the development of the NAO depends on synoptic scale wave breaking. They found that anticyclonic wave breaking is associated with the positive phase of the NAO and cyclonic wave breaking with the negative phase. Successive upstream wave breaking is responsible for the maintenance of the event. The phases of the winter NAO are also found to be associated with shifts in the storm tracks (Rogers, 1990; Hurrell, 1995). The dependency of the development of the NAO on the eddy fluxes characterises it as a phenomenon associated with non-linear processes. Li et al. (2007) conclude, by imposing an idealised forcing on a linear baroclinic model, that transient eddy forcing induces the NAO dipole with a preferred location at the exit of the Atlantic jet stream.

Apart from the known extratropical origin of the NAO, there are also studies that show the importance of the tropical impact on the NAO. They suggest that tropical variability is an important source for forcing the prevailing wintertime extratropical patterns and atmospheric trends (Sardeshmukh et al., 1987; Lin et al., 2002; Lu et al., 2004; Selten et al., 2004 and more). Changes in the tropical SSTs can excite Rossby waves that can propagate from the tropics to the extratropics creating teleconnection patterns (Hoskins and Karoly, 1981; Hoskins and Ambrizzi, 1993). It is argued that the upward trend of tropical-wide SSTs projects onto the polarity of the NAO (Hoerling et al., 2004; Hurrell et al., 2004). Peterson et al. (2002) used a dry primitive equation model forced with diabatic heating in the tropics and extratropics to find that, although the

*Corresponding author.
email: iris.manola@knmi.nl

Citation: Tellus A 2013, **65**, 19741, http://dx.doi.org/10.3402/tellusa.v65i0.19741

overall influence of the extratropics is stronger, the trend in the NAO is related to the tropical forcing. Greatbatch et al. (2012), in order to analyse the interannual trend of the NAO, applied a relaxation technique to argue that on timescales larger than 21 yr the tropics are influential, while for shorter timescales the extratropics and the stratosphere are the major sources of variability.

Along the tropical belt there are preferred regions where the SST forcing projects more strongly onto the NAO. The phase of the NAO is related to the region of tropical forcing according to Cassou (2008). Positive NAO events mostly respond to Madden–Julian Oscillation disturbances in the western-central tropical Pacific, while negative NAO events are found to be influenced by the eastern tropical Pacific-western Atlantic, leading to changes along the North Atlantic storm track. Tropical Atlantic SST anomalies are found to induce a significant NAO dipole in late winter simulations but not in early winter (Peng et al., 2005). Another study by Okumura et al. (2001) shows that tropical Atlantic forcing creates a barotropic teleconnection pattern projecting onto the NAO. The importance of the Indian Ocean is pointed out by Hoerling et al. (2004). They used enhanced SSTs over the Indian Ocean, resembling the observed warming since 1950 to force a coupled model and concluded that Indian Ocean warming projects strongly onto the positive NAO (see also Lu et al., 2004).

Here, we aim to study the atmospheric forcing of the NAO with a focus on the tropics. Feldstein (2003) suggests that the NAO has an intrinsic timescale of about 10 d. However, the Rossby wave source (RWS; see Sardeshmukh et al., 1987), which is an estimate of the driving force from the tropics, and the consequent propagation of anomalies towards the extratropics, has a longer time scale. Indeed, for the timescale of 1–10 d in boreal winter a selection of positive and negative NAO events is made (see Section 2 for the definition of the NAO events) and for these events the composites of RWS anomalies are computed, there are almost no pattern similarities between the RWS patterns for the two NAO phases. This indicates that for timescales shorter than 10 d the NAO is mainly driven by the extratropics and the influence of the tropics is negligible. Because our focus is on the impact of the tropics, timescales shorter than 10 d are excluded in this study.

For the timescale of 10–60 d the equivalent RWS composites are shown in Fig. 1 (see Section 3 for details). For the two NAO phases, the RWS anomalies show a similar structure with opposite sign and the patterns are -0.67 correlated in the areas of high significance. This anti-correlation of the RWS suggests a hypothesis that the NAO can affect the dynamical tropical forcing. Later in this paper this hypothesis is verified. These tropical changes subsequently may affect the extratropical circulation and can be of importance for the formation of the NAO patterns. In addition, the stationary winter Rossby wave patterns develop within this timescale. Finally, this time scale also captures the intraseasonal variability in tropical convection which is an effective source of Rossby waves and excludes higher frequency phenomena such as breaking waves along the storm tracks and other transient eddies that make the flow sharper and more scattered, while their important impact on the larger scale is still evident.

Prompted by the above observations we attempt to quantify the tropical impact onto the NAO in addition to the dominant extratropical forcing within the timescale of 10–60 d, using extreme positive and negative NAO events in a barotropic model. We use the barotropic model as a diagnostic tool assuming that the dynamics of the NAO is equivalent barotropic. The NAO patterns are interpreted in meridional wind anomalies in order to highlight the wave-like structure of the NAO, similarly to Branstator (2002)

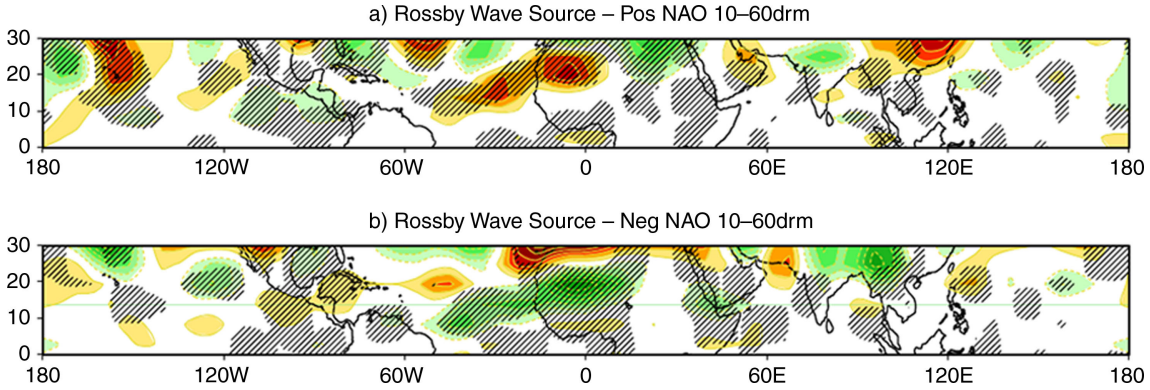

Fig. 1. Composites of RWS anomalies at 300 hPa for a) positive and b) negative NAO event days from 10–60 d means of DJF months for the period 1979–2010 using ERA–Interim data. The contour interval is $7{\cdot}10^{-12}s^{-2}$. Negative values are shown in green. The hatched black lines indicate the areas exceeding the level of 99% significance.

and Watanabe (2004). The linearity of the tropical and extratropical influence for the two phases is also discussed. Finally an effort is made to investigate whether there are preferred longitudinal regions in the tropics that force the NAO.

The paper is structured as follows. In Section 2, the data and the definition of the NAO events are introduced and the characteristics of the composites of the events are displayed. In Section 3, we focus on the possible observational tropical and extratropical forcing sources. In Section 4, the model and the experiment are described. The results of the model simulations are presented in Section 5 and in Section 6 a summary and discussion finalise this work.

2. The NAO events

2.1. Characterisation of the NAO events

We use the ERA-Interim reanalysis data (Dee et al., 2011) for Northern Hemisphere December–January–February months (DJF) from 1979 to 2010 and focus on the 10–60 d time scale. This time filtering was obtained by subtracting the 60 d running mean from the 10 d running mean. To retain the daily cycle the daily climatology was added to the resulting time series. The running means were applied over the period 1 December–28 February. For winds, we used the 300 hPa level which is a good compromise between the Rossby wave propagation level (optimum at 200 hPa) and the equivalent barotropic level at about 350 hPa, (Hoskins and Ambrizzi, 1993; Ting, 1996).

The NAO index is defined as in Branstator (2002), i.e. the first EOF of the stream function at 850 hPa. The domain used is the Atlantic sector from 90° W to 30° E over the Northern Hemisphere. The leading EOF explains 35% of the total variance. The timescale of the index is similarly 10–60 d, while extra smoothing with a Hanning window of 11 d was needed in order to select the NAO events. The selection of the positive (negative) NAO events was based on the following criteria: the NAO index increases (decreases) monotonically for 1 week to reach a value above one standard deviation (below minus one standard deviation) at least for 1 d and then decreases (increases) monotonically for the following week. From the event the middle day, which is the day with the maximum (minimum) index is selected. With this method 63 positive and 56 negative events are identified during the 32 winters.

2.2. The NAO patterns

The composites of the total wind and meridional wind anomalies of the positive and negative phase events at 300 hPa are shown in Fig. 2. The most pronounced differences are found over the North Atlantic. During the positive NAO phase the North Atlantic jet stream, indicated by the total wind speed (Fig. 2a), is shifted northward and tilted southwest–northeast towards Northern Europe and is clearly separated from the subtropical Asian jet. Over the same region the negative phase (Fig. 2b) is accompanied by a shorter Atlantic jet, more zonally oriented, situated at a more southern latitude in the subtropics and more closely connected to the Asian jet.

The meridional wind anomalies associated with both phases of the NAO (Fig. 2c and 2d) display a rather similar pattern with opposite sign and a spatial correlation in the extratropics of -0.76. They consist of a mid-latitude wavetrain with wave number 4–5, where the dominant part begins at the North American west coast and ends at the Arabian peninsula. The strongest anomaly is centred at the North mid-east Atlantic and is positive (negative) for positive (negative) NAO. The geopotential height anomalies at 500 hPa, showing the well-known dipole NAO pattern are denoted by black contours. The patterns of the two NAO phases do not exactly mirror each other, suggesting that there should be differences in the dynamics that generate these phases (see also Peterson et al., 2002; Cassou et al., 2004; Greatbatch and Jung, 2006).

3. Sources of NAO forcing

3.1. Tropics: Rossby wave source

As stated in the Introduction, anomalous divergence can force a Rossby wave–train from the tropics to the extratropics. The anomalous divergence can be created by tropical anomalous SSTs and diabatic heating.

The Rossby wave source in an equivalent barotropic atmosphere assuming negligible vertical advection and twisting terms may be approximated as

$$S = -\nabla \cdot (\zeta + f) V_\chi, \tag{1}$$

where ζ is the relative vorticity, f the Coriolis parameter and V_x the divergent component of the horizontal wind.

In Fig. 1 the Rossby wave source anomalies for positive and negative NAO events are depicted. Distinct anomalies of regional scale are shown that are well structured, especially at higher latitudes. The pattern is similar and of opposite sign for the two phases. The areas of high significance are -0.67 correlated. The significance is computed with a Student's t-test. The magnitude of the anomalies is rather uniformly spread indicating that the tropical NAO forcing is not strongly constrained to specific longitudinal regions, except for the East Atlantic and East Pacific/Caribbean where the anomalies are somewhat larger. This is further examined in Section 5.3.

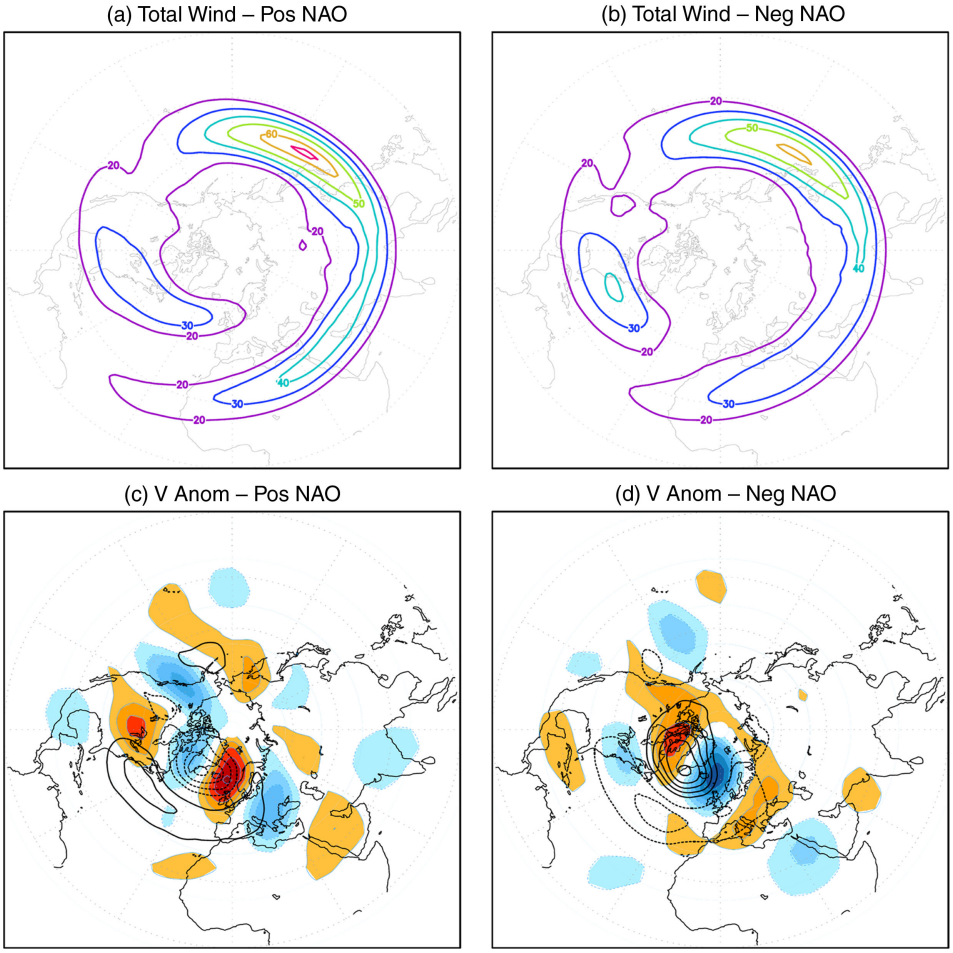

Fig. 2. Panel a) is the composite of total wind speed for positive NAO events and b) for negative events. The contour interval is 10 m/s. Composites of the meridional wind anomalies are shown in c) for positive and in d) for negative NAO events. The contour interval is 1m/s and negative values are indicated in blue colours. Over the meridional wind anomalies the geopotential height anomalies at 500 hPa are plotted. The contour interval is 35m and the negative values are indicated with dashed contours.

3.2. *Extratropics: eddy activity forcing*

The NAO in the extratropics is mainly forced by eddy activity. The highest eddy activity is found along the extratropical storm tracks. Shifts in the storm tracks are essential for the establishment and maintenance of the stationary wave patterns that create teleconnections such as the NAO. It should be noted that the state of the NAO can influence back the eddy activity, but here we focus on the one-way relationship.

The contribution of the eddy activity to the time mean flow can be computed straight forwardly by applying Reynolds decomposition to the momentum equations (Kok and Opsteegh, 1985):

$$F_{\mathrm{Ex}} = -\left(\frac{1}{\alpha\cos\phi}\frac{\partial\overline{u'2}}{\partial\lambda} + \frac{1}{\alpha}\frac{\partial\overline{u'v'}}{\partial\phi}\right), \tag{2}$$

and

$$F_{\mathrm{Ey}} = -\left(\frac{1}{\alpha\cos\phi}\frac{\partial\overline{u'v'}}{\partial\lambda} + \frac{1}{\alpha}\frac{\partial\overline{v'2}}{\partial\phi}\right), \tag{3}$$

where we have neglected the curvature and the vertical advection terms. The overbars denote the time means and the primes denote the anomalies. By applying the rotation operator on eqs. (2) and (3), they can be transformed into a vorticity forcing for a barotropic atmosphere:

$$F_{\mathrm{EV}} = \frac{1}{\alpha}\frac{\partial F_{\mathrm{Ex}}}{\partial\phi} - \frac{1}{\alpha\cos\phi}\frac{\partial F_{\mathrm{Ey}}}{\partial\lambda}, \tag{4}$$

We have evaluated eq. (4) using 6-hourly ERA-Interim data for positive and negative NAO events at 500 hPa, which is an appropriate level for addressing baroclinic eddy activity. The anomalies are computed with respect to a 30-d

running mean. The differences in the eddy forcing of the barotropic atmosphere between positive and negative NAO composite events are displayed in Fig. 3. Coherent differences are shown between the two phases. The largest among them are found over the Atlantic, the East Pacific/American continent and the Antarctic. Further discussion of this figure follows in Section 5.1

4. Model and experimental set up

The teleconnections associated with the NAO that are initiated in the tropics by the RWS are thought to be governed by equivalent barotropic dynamics. The extratropical transient eddy activity and wave breaking that influence the generation and maintenance of NAO is a baroclinic process acting on a regional scale with a timescale of 2–5 d. In this study, we are however interested in the timescales of 10–60 d. For these spatial and time scales, the impact of the eddies can be assumed to be equivalent barotropic. Therefore we use a barotropic model as a diagnostic tool to quantify the influence of tropical and extratropical sources of the NAO. A benefit from working with the barotropic model is that it provides a transparent framework for interpreting the results. Watanabe (2004) also used a barotropic model to examine the zonally oriented wavetrains associated with the NAO that are concurrent with RWS anomalies.

The barotropic vorticity equation (BVE) describes the evolution of the flow of a barotropic fluid on a rotating sphere:

$$\frac{d\zeta}{dt} = \frac{\partial \zeta}{\partial t} + J(\psi, \zeta + f) + \lambda\zeta + \mu\nabla^4\zeta = F, \tag{5}$$

where ψ is the stream function, ζ is the relative vorticity, f the Coriolis parameter, λ the Ekman pumping linear coefficient and μ the super viscosity. The BVE is solved on the sphere by a spectral model with a triangular truncation of T21. The forcing F is determined as such that the background flow remains stationary ($\frac{\partial \zeta}{\partial t} = 0$). The coefficients λ and μ are set to 9 and 3 d, respectively, to keep the flow stable.

The BVE is applied to the stream function of NAO composites of positive and negative events and also to the mean state of all 32 winters using 10–60 d running means of ERA–Interim wind data at 300 hPa.

The forcing that keeps the time mean winter (DJF) flow stationary is denoted as F_0. The forcings that keep the positive and negative NAO composite fields stationary are denoted as $F_{\mathrm{NAO}}{}^{+}$ and $F_{\mathrm{NAO}}{}^{-}$, respectively. These NAO forcings can be decomposed into a mean and an anomalous forcing:

$$F^{+}_{\mathrm{NAO}} = F_0 + F^{+\prime}_{\mathrm{NAO}}, \tag{6}$$

and

$$F^{-}_{\mathrm{NAO}} = F_0 + F^{-\prime}_{\mathrm{NAO}}, \tag{7}$$

By restricting the anomalous NAO forcings ($F^{+\prime}_{\mathrm{NAO}}$ and $F^{-\prime}_{\mathrm{NAO}}$) to the tropics (0°–30° N) or the extratropics (30°–90° N) and running the BVE to equilibrium the impact of the tropical and extratropical part of the NAO forcings can be evaluated. This approach is, however, only valid if the response to the anomalous forcing is to first order linear. The response to the tropical and extratropical forcing can then be linearly added. We have tested the linearity by comparing the total response with the summation of the tropical and the extratropical response. The differences between these responses are indeed small, as will be discussed in Section 5.2.

To assess the tropical and extratropical contribution to the teleconnections for each phase the weighted Kinetic Wave Energy Anomaly is computed using the meridional wind:

$$\frac{1}{N}\Sigma(V_{eq} - V_0)^2, \tag{8}$$

where V_{eq} is the meridional wind after the model has reached the equilibrium state and V_0 the meridional wind of the composite of all 32 winters. Σ indicates the summation over all grid points (N).

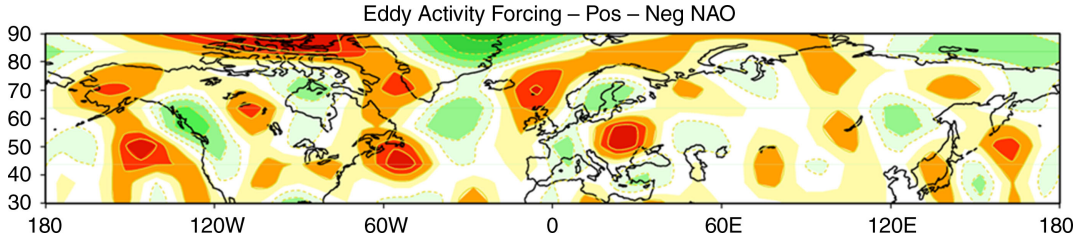

Fig. 3. Anomalies of eddy activity forcing composites of positive minus negative NAO events. The data are derived from zonal and meridional wind anomalies from ERA–Interim of DJF 1979–2010 yr. The contour interval is $6{\cdot}10^{-12}s^{-2}$ and the green colour shades indicate negative values.

5. Tropical and extratropical influence on NAO patterns

5.1. *Model-derived barotropic vorticity forcing*

The anomalous vorticity forcing for the two NAO phases [$F^{+\prime}_{\mathrm{NAO}}$ and $F^{-\prime}_{\mathrm{NAO}}$, see eqs. (6) and (7)] are computed in the barotropic model for the tropics and the extratropics. They are displayed in Fig. 4. In order to verify that the BVE can be used to evaluate the dynamics of the NAO, the patterns of the model vorticity should bear resemblance to the observational forcings. However, the RWS and eddy forcing are approximations of the actual NAO forcing of the barotropic flow at one level. The forcing of the NAO in the tropics by the generation of Rossby waves that propagate to the extratropics occurs mainly in the upper troposphere. In the extratropics, these Rossby waves lose their baroclinic structure and become predominantly equivalent barotropic. Similarly the amplitude of the eddy forcing varies strongly with height. Due to these approximations a direct agreement in amplitudes should not be anticipated and we will mainly concentrate our analysis on pattern comparison.

For both phases of the NAO there is reasonable agreement between the anomalous model tropical vorticity

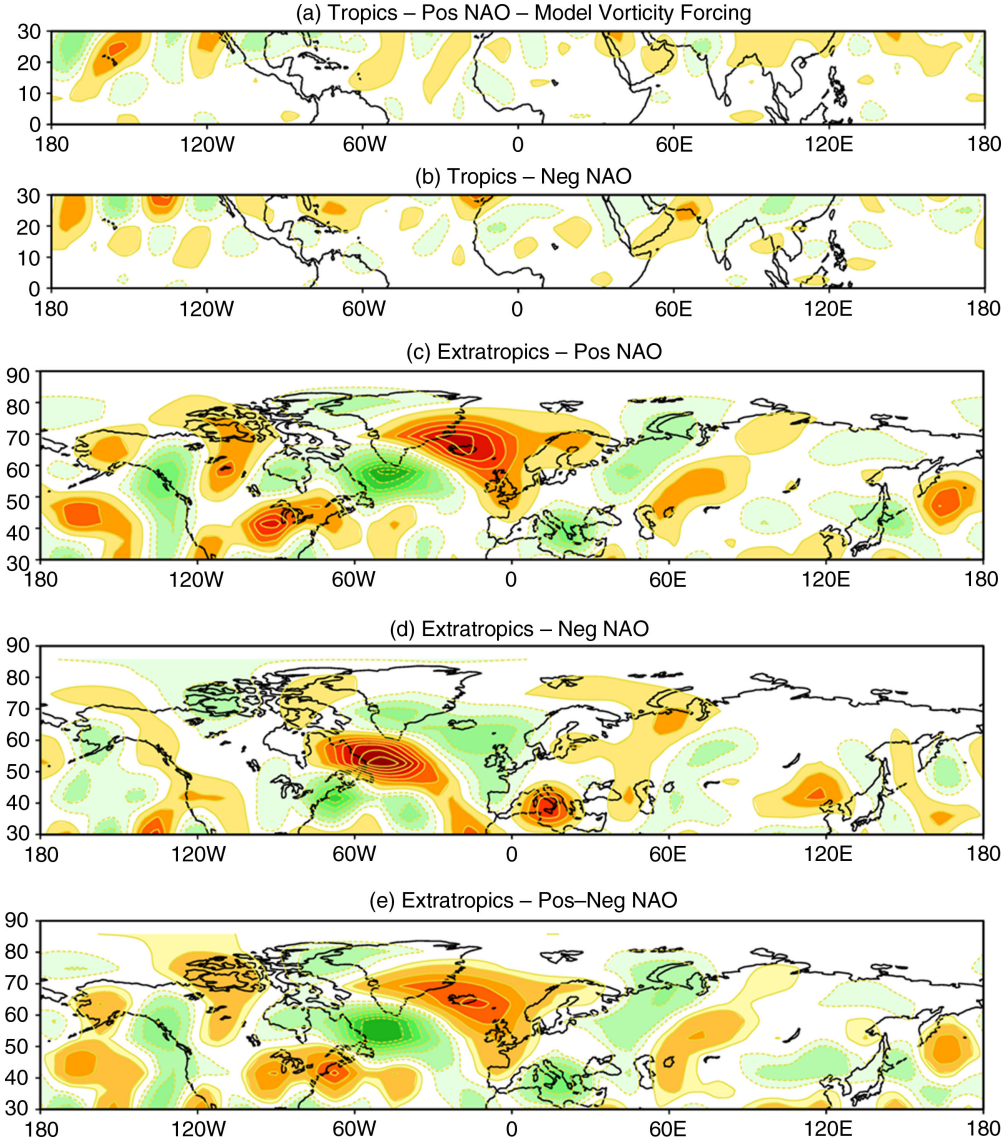

Fig. 4. Composites of anomalous vorticity forcing computed in the model by solving the BVE for a) the tropics (0°–30°*N*) for positive NAO events, b) for negative NAO events and for c) the extratropics (30°–90°*N*) for positive events and d) for negative events. At e) are the differences between positive and negative extratropical forcing. The contour interval is $4{\cdot}10^{-12}s^{-2}$. Negative values are indicated in green.

forcing (Fig. 4a and 4b) and the observed RWS (Fig. 1) in sign and location of the pattern.

Similarly to the tropical forcing, the extratropical model vorticity forcing for positive NAO (Fig. 4c) has the opposite sign of the forcing for the negative NAO (Fig. 4d). The anomalies in Fig. 4e are compared to the anomalous observational eddy activity forcing in Fig. 3. Although the discrepancies are somewhat larger, there are still some similarities, especially over the Atlantic and E. Pacific-American continent where the largest values are found. There both patterns show a similar Southwest-Northeast chain of anomalies.

The above results indicate that the BVE, despite its approximations, can be used to evaluate the dynamics of the NAO. In addition, it is confirmed that the major forcing of the NAO in the extratropics is caused by eddy forcing, whereas in the tropics it is dominated by the RWS. The ability of the BVE to present the dominant forcing in the tropics as well as the extratropics motivated us to use the BVE to analyse the impact of the tropical RWS forcing and to compare it with the extratropical eddy forcing. This is further discussed in the following paragraphs.

5.2. *Assessing the tropical and extratropical impact*

To investigate the impact of the tropical and extratropical forcing on generating NAO events the mean state of the atmosphere is forced in the barotropic model with the F'_{NAO} confined to 0°–30° N or 30°–90° N, respectively, for both positive and negative NAO events. The model is run to equilibrium. The meridional velocity anomalies from the simulations are shown in Fig. 5. For each NAO phase, firstly, only the response to tropical forcing is shown, then only the response to extratropical forcing and finally the response to tropical and extratropical forcing together.

A surprising result is that the responses to tropical and extratropical forcing have a similar structure but are of opposite sign. The tropical forcing thus reduces the

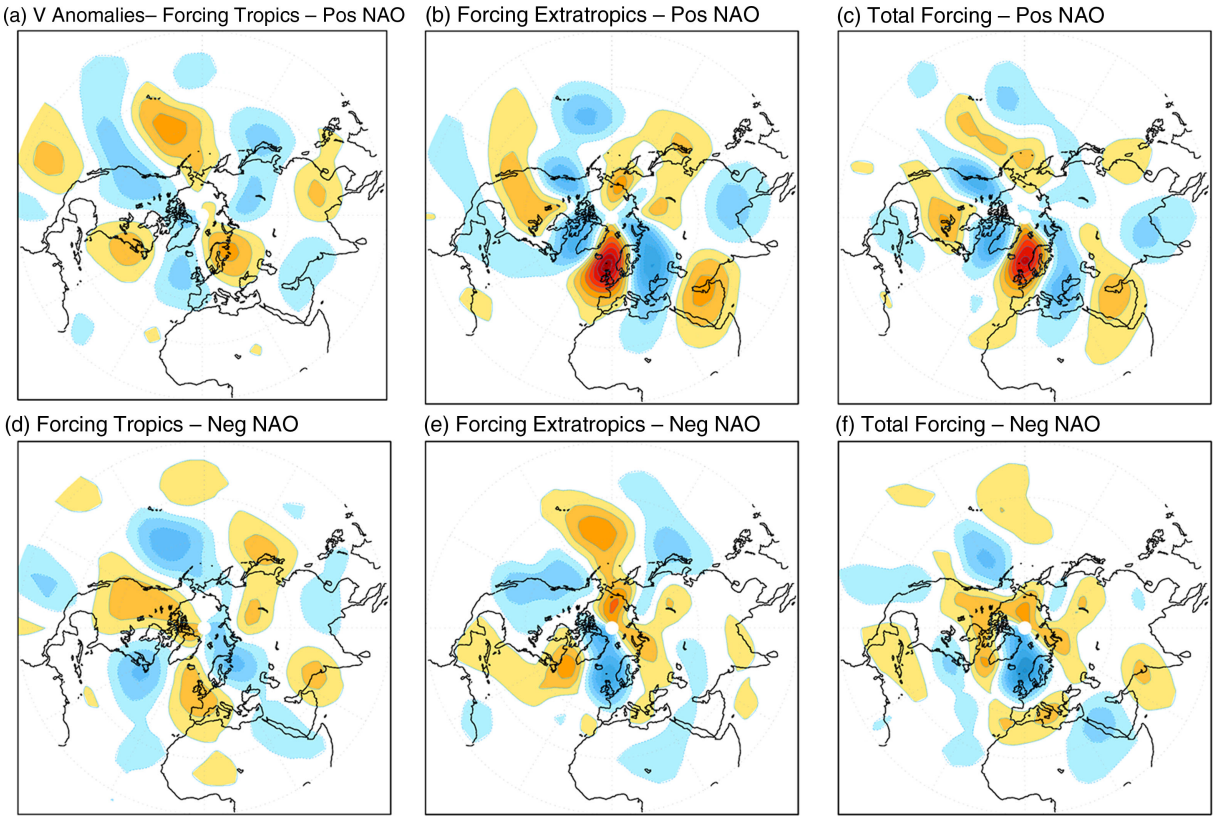

Fig. 5. Meridional wind anomalies simulated by the barotropic model when the mean circulation at 300 hPa is forced with the anomalous $F'_{\mathrm{NAO}}$and run to equilibrium. First the forcing is restricted to the tropical band (0°–30°N, left panels), where in panel a) the positive NAO forcing ($F'_{\mathrm{NAO+}}$) is used and in d) the negative NAO forcing is used ($F'_{\mathrm{NAO-}}$). Second, the forcing is applied only in the extratropics (30° – 90°N, middle panels), similarly in b) the positive NAO forcing ($F'_{\mathrm{NAO+}}$) is used and in e) the negative NAO forcing is used ($F'_{\mathrm{NAO-}}$). Finally to show the overall effect of using the anomalous NAO forcing, the entire hemisphere is forced, in c) with $F'_{\mathrm{NAO+}}$ and in f) with $F'_{\mathrm{NAO-}}$. The contour intervals are 1 m/s and negative values are indicated in blue.

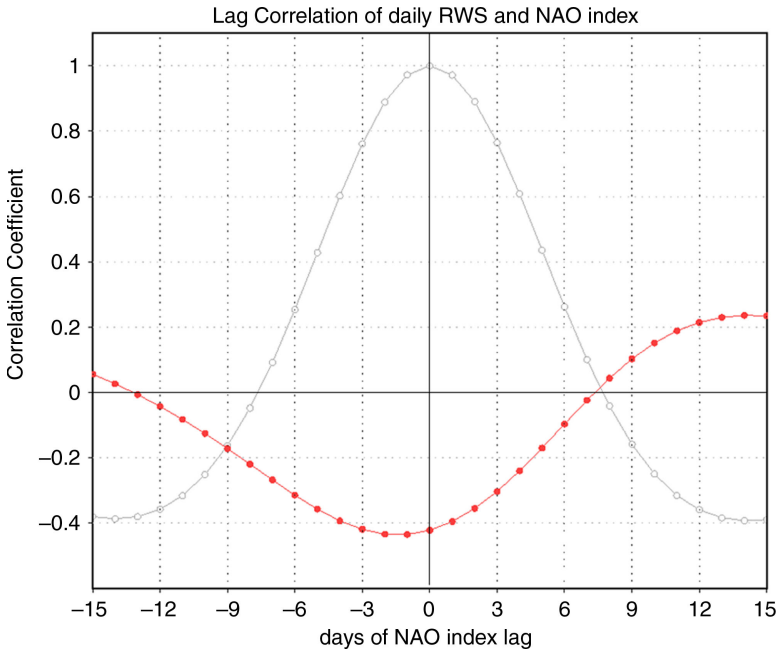

Fig. 6. Red line: a lead-lag correlation of the daily RWS index and the NAO index for DJF. The RWS index is defined as the projection of the daily RWS associated with the NAO on the total RWS composite. Grey line: an autocorrelation of the NAO index. The horizontal axis denotes the lag in days of the NAO index. The vertical axis is the correlation coefficient between lagged NAO index and RWS index, or the autocorrelation coefficient of the NAO index.

response of the extratropical forcing. To further analyse this we have performed a lead/lag analysis between daily RWS and the NAO index, which is shown in Fig. 6. It reveals that the RWS is negatively correlated with the NAO and that it lags the NAO index by 2 d. This time scale is related to the time necessary for the NAO to affect the tropical circulation. For large positive and negative lags, the correlation becomes approximately zero. In addition, the autocorrelation of the NAO, also shown in Fig. 6, reveals that RWS-NAO correlation has a similar damping time scale as that of the NAO. Also, the RWS-NAO becomes approximately zero when the NAO autocorrelation vanishes. We therefore conclude that the damping of the NAO by the tropical forcing is due to a negative feedback of the tropical circulation in response to the NAO that is generated in the extratropics. Earlier studies have established the connection between the NAO and the circumglobal wave guide. Watanabe (2004) has found events where anomalous convergence is established at the entrance of the Asian jet that lag the peak of the NAO by 2 d. This signal is associated with the decay of the NAO and subsequently propagates further downstream thereby affecting the convection on a global scale. Another hypothesis is that the trade winds associated with the Azores high can affect subtropical SSTs and through the wind-evaporation-SST feedback the ITCZ (Chang et al., 1997). We speculate that these mechanisms might provide the negative feedback that we encountered.

To quantify the damping of the tropical forcing with respect to the extratropical forcing of the NAO, the kinetic wave energy anomaly [KWE, eq. (8)] is computed over the Atlantic region between 30° N and 90° N. The KWE resulting from tropical forcing simulations alone is compared only to that resulting from the extratropical forcing only: for the positive NAO phase the tropics comprise the 14% of the KWE sum and the extratropics the rest with 86%. Compared to the positive phase, the negative phase shows enhanced tropical contribution (35%) with respect to the extratropics (65%). The above percentages are positive numbers, since the wave energy by definition is positive. Therefore it indicates only the amplitude of the influence. It should be noted that the tropical and extratropical KWE cannot be added linearly as they are quadratic quantities. The sign of the influence depends on the sign of the meridional wind anomalies, compared to the total response as seen in Fig. 5. Since the tropical forcing response is mainly of opposite sign to the extratropical forcing we conclude that by this percentage the tropics are damping the dominating extratropical response and reducing the amplitude of the total NAO pattern.

The non-equal contribution of the two phases is a sign of non-linearity of the NAO. This is due to the different

Table 1. At the left hand side the ratios of the contribution of the tropics and the extratropics for the positive and negative NAO phases are shown, quantified by the kinetic energy anomaly [eq. (8)]. At the right hand side is the zonal average of the absolute vorticity forcing F'_{NAO}, showing that the negative NAO tropical model vorticity forcing is about 14% higher in ratio between tropical–extratropical forcing than the positive phase

	Contribution		Vorticity forcing ($10^{-11}s^{-2}$)	
	Tropical	Extratropical	Tropical	Extratropical
Pos NAO	14%	86%	1.22	3.4
Neg NAO	35%	65%	1.22	2.99

amplitudes of the extratropical forcing during the positive and negative NAO, as is seen in Table 1. The amplitudes are computed as the zonal average of the absolute vorticity forcing $F\prime_{NAO}$. The extratropical forcing of the positive phase is about 14% stronger than that of the negative phase, explaining why the extratropics in the positive phase play a more dominant role compared to the negative. The tropical forcing is of similar amplitude for the selected NAO events.

Peterson et al. (2002), in order to assess the non-local influence on the low-frequency behaviour of the NAO, forced a primitive AGCM with a derived adiabatic forcing only in the tropics and the extratropics, respectively. In their Fig. 3a and 3b, the SLP differences between two periods over the Northern Hemisphere are shown when only the tropics or extratropics are forced. The patterns bear significant resemblance to our barotropic model results, indicating that indeed the dynamics can be captured by the BVE. From these figures we can also observe that forcing in the tropics results in a pattern of opposite sign to forcing in the extratropics. They also correlated the NAO index when forcing in only the tropics or extratropics with the observed index and found a correlation of 0.39 for the tropical forcing and 0.55 for the extratropical forcing.

The similarities between the observed meridional wind anomalies as seen in Fig. 2c and 2d with those reconstructed in the model by the summation of the tropical and extratropical patterns in Fig. 5c and 5f confirm that the model non-linearities do not play an important role in the simulation. Some discrepancies, mostly seen on the negative phase, can be due to numerical model approximations or non-linearities.

To further validate the results, the simulations are repeated, but instead of the model computed barotropic vorticity forcing we used the observed RWS [eq. (1)] as the tropical forcing and the eddy activity [eq. (4)] as the extratropical forcing. The results are shown in Fig. 7. Comparison of Fig. 5 with Fig. 7 (7a and 7c with 5a and 5d, and 7b and 7d with 5b and 5e, respectively) reveals that they bear significant spatial similarities. The amplitude of the response for the observed RWS is somewhat reduced compared to the model response, whereas for the eddy forcing it is somewhat enhanced, but still comparable. This agreement indicates that there is a direct connection between tropical observed RWS and the model barotropic vorticity forcing and also between the extratropical observed eddy activity and the barotropic model forcing.

5.3. *Tropical forcing: zonal dependency*

To assess whether there are preferred tropical regions that project stronger on the NAO, the model is forced at constrained longitudinal regions with the observed anomalous RWS. The selected forcing regions are those where the RWS shows maximum amplitude and significance (see Fig. 1). They are the East Atlantic, East Pacific/Caribbean, Middle Pacific and East Indian Ocean. The width of the tropical 0°–30° N forcing window is 40°. Comparison of the response to local forcing in Fig. 8 with the hemispheric-wide tropical forcing in Fig. 5a and 5d shows that depending on the region of the forcing the excited patterns show differences, but overall the main structure for each case bears some resemblance to the pattern of the hemispheric-wide forcing.

As discussed in Section 5.2, the sign of the response to the hemispheric-wide tropical forcing is opposite to the response of the total forcing, indicating that the hemispheric-wide tropical forcing tends to reduce the impact of the extratropical forcing. However, when the forcing is on a regional scale the sign of the response depends on the sign of the local forcing. An example for the positive NAO is the response to the local forcing over the East Pacific/Caribbean and over the Eastern Atlantic (Fig. 8c and 8e). The response to these forcings is opposite, in agreement with the opposite sign of these forcings. The RWS forcing is negative over the East Pacific/Caribbean and positive over Eastern Atlantic (Fig. 1). The sign of response of the later agrees with that of the total NAO. We therefore conclude that areas that enhance the strength of the total NAO are those of negative RWS.

The amplitude of response, apart from the location of the source, depends linearly on the amplitude of the source itself. This is illustrated in Fig. 8c and 8d, where the forcing for the positive phase over the E. Pacific/Caribbean is rather weak, and in agreement with the response, contrarily to the negative phase where the forcing is rather strong. Cassou (2008) also notices that the two phases of the NAO respond to forcing on different locations in the tropics.

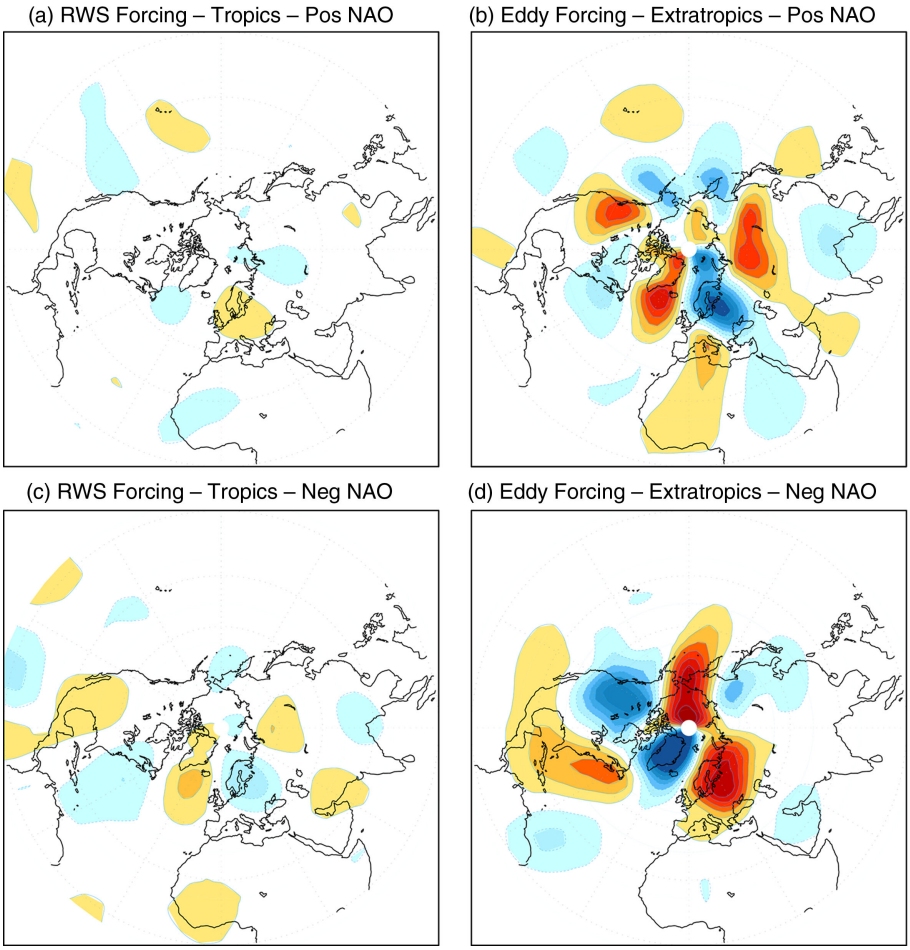

Fig. 7. Similar to Fig. 5 but instead of the model vorticity forcing, the observational forcing is applied. At a) is the response to the observed tropical RWS forcing for positive NAO events and c) for negative NAO events. In b) the forcing is the extratropical observed eddy activity for positive NAO and in d) for negative NAO. The contour intervals are 1 m/s and negative values are indicated in blue.

Combination of both divergent and convergent vorticity forcing can interfere destructively and result in a response of smaller amplitude, as seen in Fig. 8h, compared to Fig. 8g. The absolute responses to the forcing of the selected tropical areas in terms of kinetic wave energy are listed in Table 2.

There are non-linearities with respect to the sign and location of the forcing. The same areas forced with the opposite phase do not give exact mirroring patterns. Similar results concerning non-linearities with respect to the sign of the tropical forcing on the extratropical circulation have been noted by Kushnir and Lau (1992), Robinson et al. (2003) and Li et al. (2007).

6. Summary and conclusions

In this study we investigated the contribution of tropical and extratropical forcing on the formation of the different phases of the NAO pattern. While many previous studies on this subject focused on interannual and longer term variability (Thompson et al., 2003; Hurrell et al., 2004; Li et al., 2007), we focus on the relatively short 10–60 d time scale. That is, we are interested in the actual NAO events, rather than the stationary wave response to remote and local forcing. This is motivated by the time scale of the development of an NAO event which is thought to be associated with triggering and propagation of Rossby waves from the tropics to the extratropics and with eddy activity in the mid-latitude jet (Feldstein, 2003; Franzke et al., 2003). Analysis of the NAO forcing in the tropics for timescales shorter than 10 d indicated that the tropics are rather insignificant for the NAO. Because a main focus was the tropical forcing of the NAO, those frequencies are excluded. We checked that the NAO characteristics for the 10–60 timescale were not very different from those of the 1–10 d timescale.

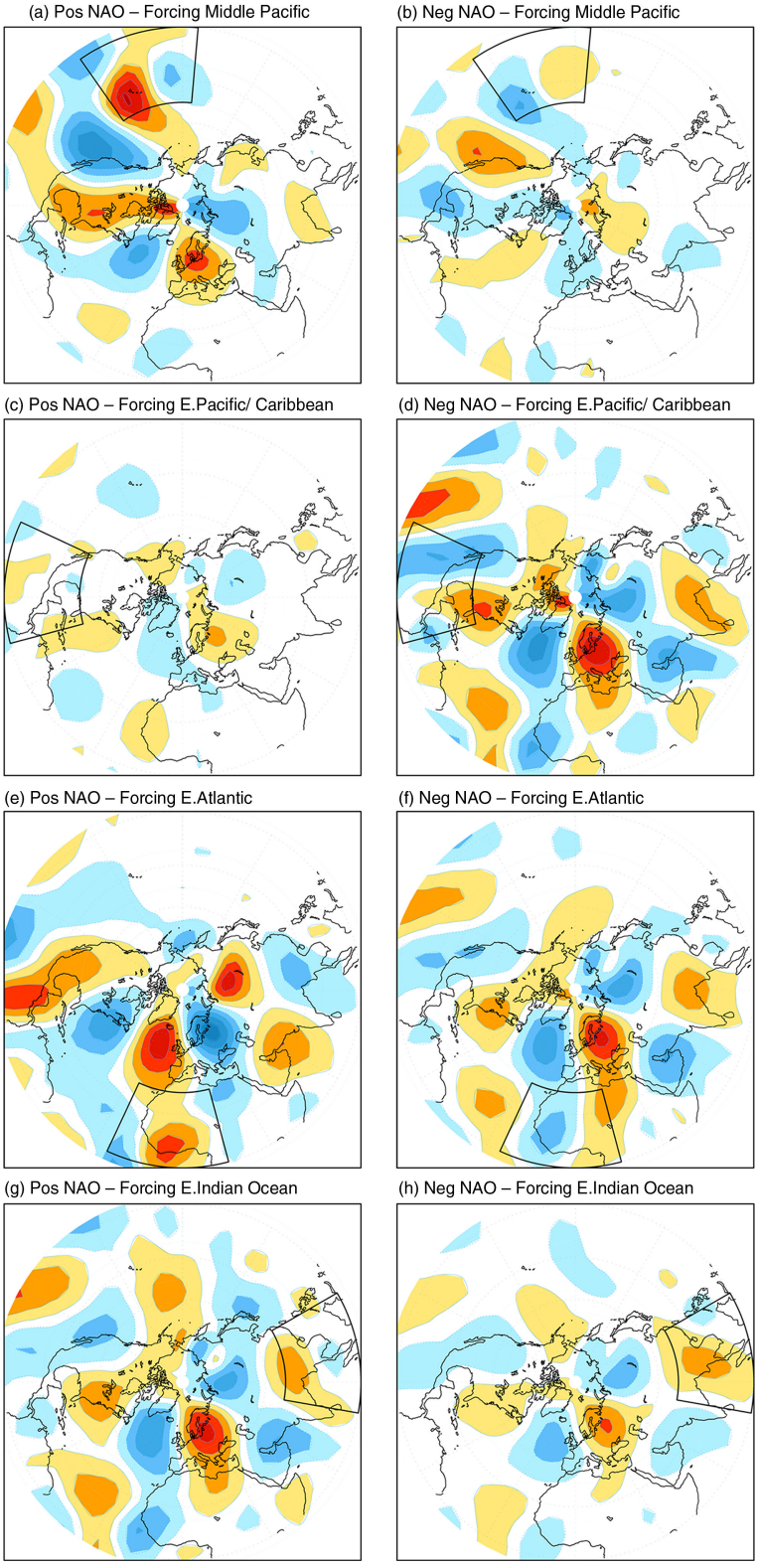

Fig. 8. Meridional wind anomalies simulated by the barotropic model when forced with the observed RWS anomalies in the tropics (0°–30°*N*) in constrained regions of 40°longitude. Left column for the positive NAO phase and right column for the negative phase. The forced regions are indicated by a black box. The contour intervals are 0.5 m/s and negative values are indicated in blue.

Table 2. The kinetic wave energy anomaly as a response to forcing on the selected tropical regions for the positive and negative NAO phases

	Kinetic wave energy (m^2/s^2)			
	Mid. Pacific	E. Pacific/ Caribbean	E. Atlantic	E. Indian Ocean
Pos NAO	0.46	0.08	0.63	0.49
Neg NAO	0.16	0.63	0.42	0.19

We use a barotropic model to diagnose the contribution of local and remote forcing to the formation of NAO events. The barotropic model allows us to study the contribution of estimates of the observed vorticity forcing in the atmosphere directly. The model also allows us to compute the anomalous forcing associated with the NAO inversely. This approach is more direct than prescribing anomalous SST conditions or idealised diabatic heating patterns in a general circulation model.

We made composites of the NAO to characterise the atmospheric flow and computed the vorticity forcing terms using atmospheric reanalysis data filtered between 10–60 d. The positive phase of the NAO is associated with a northward shift and southwest–northeast tilt of the mid-latitude jet and the negative NAO with a zonally oriented jet. The meridional velocity anomalies at 300 hPa show a clear wavetrain. The vorticity forcing shows distinct patterns of opposite sign for both NAO phases. It is encouraging that the inversely determined forcing bears resemblance with estimates of the vorticity forcing from reanalysis data. This indicates that the barotropic model can be used to diagnose the impact of local and remote forcing. Note that exact comparison is not possible. For instance, choices had to be made as to which levels to consider when computing forcing from reanalysis data.

By applying vorticity forcing in the barotropic model associated with both phases of the NAO for the extratropics and tropics, respectively, and comparing the results with a simulation with the total forcing we could quantify the impact of different regions. Fourteen percent of the meridional velocity variance at 300 hPa in the positive NAO phase could be generated by tropical forcing only. This number increases to 35% for the negative NAO phase, consistent with a relatively larger tropical vorticity forcing compared to the extratropical forcing. The patterns resemble those of Peterson et al. (2002) who focused on the stationary wave response. An important result is that the average tropical forcing appears to reduce the amplitude of the existing meridional wind anomaly pattern that is associated with the NAO. This is confirmed by a lead/lag correlation analysis showing that the NAO precedes the tropical forcing by 2 d. A physical mechanism for such a response is yet unclear. Analysis of forcing from distinct regions in the tropics shows that both strengthening and damping can be found. When evaluating the impact of extratropical forcing, some care must be taken because of the non-linear interactions between the NAO and the eddy momentum fluxes.

These results indicate a pronounced impact of tropical forcing on the NAO. The impact of tropical variability on the NAO has been evaluated in many studies before, but focused mostly on seasonal or longer time scales associated with changes in low-frequency behaviour of the NAO. Here we focus on actual NAO events and on time scales relevant for the atmospheric dynamics to set up the teleconnections. The results may imply that events such as the Madden–Julian Oscillation can contribute to the forcing of the NAO. Some studies have pointed in this direction as well (e.g. Cassou, 2008). This study shows that there is a damping feedback of the tropical circulation to the NAO patterns that is generated in the extratropics.

7. Acknowledgements

The authors thank Frank Selten and Will de Ruijter for the motivation and the helpful discussions. This work is part of the INATEX research program, which is financed by the Netherlands Organisation for Scientific Research (NWO). We also thank the two anonymous reviewers who provided valuable suggestions and remarks that improved the outcome of this work.

References

Benedict, J., Lee, S. and Feldstein, S. 2004. Synoptic view of the North Atlantic Oscillation. *J. Atmos. Sci.* **61**, 121–144.

Branstator, G. 2002. Circumglobal teleconnections, the jet stream waveguide, and the North Altantic Oscillation. *J. Clim.* **15**, 1893–1910.

Cassou, C. 2008. Intraseasonal interaction between the Madden-Julian Oscillation and the North Atlantic Oscillation. *Nature* **455**, 523–527.

Cassou, C., Terray, L., Hurrell, J. W. and Deser, C. 2004. North Atlantic winter climate regimes: Spatial asymmetry, stationarity with time, and oceanic forcing. *J. Climate.* **17**, 1055–1068.

Chang, P., Ji, L. and Li, H. 1997. A decadal climate variation in the tropical Atlantic Ocean from thermodynamic air-sea interaction. *Nature* **385**, 516–518.

Dee, D. P., Uppala, S. M., Simmons, A. J., Berrisford, P., Poli, P. and co-authors. 2011. The ERA-Interim reanalysis: Configuration and performance of the data assimilation system. *Quart. J. Roy. Meteor. Soc.* **137**, 553–597.

Feldstein, S. B. 2003. The dynamics of NAO teleconnection pattern growth and decay. *Quart. J. Roy. Meteor. Soc.* **129**, 901–924.

Franzke, C., Lee, S. and Feldstein, S. 2003. Is the North Atlantic Oscillation a breaking wave? *J. Atmos. Sci.* **61**, 145–160.

Greatbatch, J. R. and Jung, T. 2006. Local versus tropical diabatic heating and the winter North Atlantic Oscillation. *J. Climate*. **20**, 2058–2075.

Greatbatch, R. J., Gollan, G. and Jung, T. 2012. An analysis of trends in the boreal winter mean tropospheric circulation during the second half of the 20th century. *Geophys. Res. Lett*. **39**, L13809, DOI: 10.1029/2012GL052243.

Hoerling, M. P., Hurrell, J. W., Xu, T., Bates, G. T. and Phillips, A. S. 2004. Twentieth century North Atlantic climate change. Part II: understanding the effect of Indian Ocean warming. *Climate Dyn*. **23**, 391–405.

Hoskins, B. J. and Ambrizzi, T. 1993. Rossby wave propagation on a realistic longitudinally varying flow. *J. Atmos. Sci.* **50**, 1661–1671.

Hoskins, B. J. and Karoly, D. J. 1981. The steady linear responses of a spherical atmosphere to thermal and orographic forcing. *J. Atmos. Sci*. **38**, 1179–1196.

Hurrell, J. W. 1995. Decadal trends in the North Atlantic Oscillation regional temperatures and precipitation. *Science* **269**, 676–679.

Hurrell, J. W., Hoerling, M. P., Phillips, A. S. and Xu, T. 2004. Twentieth century North Atlantic climate change. Part I. Assessing determinism. *Clim. Dyn*. **23**, 371–389.

Kok, C. J. and Opsteegh, J. D. 1985. Possible causes of anomalies in seasonal mean circulation patterns during the 1982–83 El Nino Event. *J. Atm. Sci.* **42**, 677–694.

Kushnir, Y. and Lau, N. C. 1992. The general circulation model response to a North Pacific SST anomaly: Dependent on timescale and pattern polarity. *J. Climate*. **5**, 271–283.

Li, S., Robinson, W. A., Hoerling, M. P. and Weickmann, K. M. 2007. Dynamics of the extratropical response to a tropical Atlantic SST anomaly. *J. Clim*. **20**, 560–574.

Lin, H., Derome, J., Greatbatch, R. J., Peterson, K. A. and Lu, J. 2002. Tropical links of the Arctic Oscillation. *Geophys. Res. Lett*. **29**, 1943–1947.

Lu, J., Greatbatch, R. J. and Peterson, K. A. 2004. Trend in Northern Hemisphere winter atmospheric circulation during the last half of the twentieth Century. *J. Clim*. **17**, 3745–3760.

Okumura, Y., Xie, S.-P., Numaguti, A. and Tanimoto, Y. 2001. Tropical Atlantic airsea interaction and its influence on the NAO. *Geophys. Res. Lett*. **28**, 1507–1510.

Peng, S., Robinson, W. A., Li, S. and Hoerling, M. P. 2005. Tropical Atlantic SST forcing of coupled North Atlantic seasonal responses. *J. Climate*. **18**, 480–496.

Peterson, K. A., Greatbatch, R. J., Lu, J., Lin, H. and Derome, J. 2002. Hindcasting the NAO using diabatic forcing of a simple AGCM. *Geophys. Res. Lett*. **29**, DOI: 10.1029/201GL014502.

Platzman, G. W. 1968. The Rossby wave. *Quart. J. Roy. Meteor. Soc*. **94**, 225–248.

Riviere, G. and Orlanski, I. 2007. Characteristics of the Atlantic storm track eddy activity and its relationship with the North Atlantic Oscillation. *J. Atmos. Sci*. **64**, 241–266.

Robinson, W. A., Li, S. and Peng, S. 2003. Dynamical nonlinearity in the atmospheric response to Atlantic sea surface temperature anomalies. *Geophys. Res. Lett*. **30**, 2038.

Rogers, J. 1990. Patterns of low-frequency monthly sea level pressure variability (1899–1986) and associated wave cyclone frequencies. *J. Clim*. **3**, 1364–1379.

Sardeshmukh, P. D., Prashant, D. and Hoskins, B. J. 1987. The generation of global rotational flow by steady idealized tropical divergence. *J. Atmos. Sci*. **45**, 1228–1251.

Selten, F. M., Branstator, G. W., Dijkstra, H. A. and Kliphuis, M. 2004. Tropical origins for recent and future Northern Hemisphere climate change. *Geophys. Res. Lett*. **31**, L21205, DOI: 10.1029/2004GL020739.

Thompson, D. W. J., Lee, S. and Baldwin, M. P. 2003. Atmospheric processes governing the Northern Hemisphere Annular Mode/North Atlantic Oscillation. *Geophys Monogr*. **134**, 81–112.

Ting, M. 1996. Steady linear response to tropical heating in barotropic and baroclinic models. *Amer. Meteor. Soc*. **53**(12), 1698–1709.

Vallis, G. K., Gerber, E. P., Kushner, P. J. and Cash, B. A. 2004. A mechanism and simple dynamical model of the North Atlantic Oscillation and annular modes. *J. Atmos. Sci*. **61**, 264–280.

Watanabe, M. 2004. Asian jet waveguide and a downstream extension of the North Atlantic Oscillation. *J. Clim*. **17**, 4674–4691.